

Effect of CNT Agglomeration on the Electrical Conductivity and Percolation Threshold of Nanocomposites: A Micromechanics-based Approach

B.J. Yang¹, K.J. Cho¹, G.M. Kim¹ and H.K. Lee^{1,2}

Abstract: The addition of carbon nanotubes (CNTs) to a matrix material is expected to lead to an increase in the effective electrical properties of nanocomposites. However, a CNT entanglement caused by the matrix viscosity and the high aspect ratio of the nanotubes often inhibits the formation of a conductive network. In the present study, the micromechanics-based model is utilized to investigate the effect of CNT agglomeration on the electrical conductivity and percolation threshold of nanocomposites. A series of parametric studies considering various shapes and curviness distributions of CNTs are carried out to examine the effects of entanglement on the electrical performance of nanocomposites. Comparisons between experimental results and the present predictions are made to evaluate the predictive capability of the proposed model. In addition, the present model is incorporated into the commercial finite element software ANSYS HFSS to simulate the electromagnetic interference (EMI) shielding effectiveness of nanocomposites.

Keywords: Carbon nanotube-reinforced composites, electrical conductivity, nanotube entanglement, percolation threshold, electromagnetic interference shielding effectiveness.

1 Introduction

The electrical characteristics of carbon nanotube (CNT)-reinforced nanocomposites have attracted the interest of engineers and researchers due to their potential applications in many fields such as sensing and actuation technologies [Lau, Gu, and Hui (2006); Kim, Nam, and Lee (2014)]. The conductivity of CNTs is much higher than that of a given matrix, and therefore the addition of CNTs to a matrix is expected to improve the effective electrical performance of composites [Asgary,

¹ Department of Civil and Environmental Engineering, Korea Advanced Institute of Science and Technology (KAIST), 291 Daehak-ro, Yuseong-gu, Daejeon 305-701, Republic of Korea.

² Corresponding author. E-mail: leeh@kaist.ac.kr

Nourbakhsh, and Kohantorabi (2013)]. Once the electrical path of CNTs is developed within the matrix, the effective conductivity of the composites dramatically rises, and the specific volume fraction of CNTs is defined as the percolation threshold point [Pan, Weng, Meguid, Bao, Zhu, and Hamouda (2011); Lahiri, Ghosh, and Agarwal (2012)].

The percolation threshold of the composite containing CNTs is much lower than that of conventional fillers since the aspect ratio (length-to-diameter) of CNTs is relatively high, exceeding 100 [Deng, Zheng, Wang, and Nan (2007); Li, Thostenson, and Chou (2008)]. Although outstanding enhancement is obtained with lengthy nanotubes, the high aspect ratio of CNTs often causes nanotube entanglement by van-der-Waals (vdW) attraction, inhibiting the formation of conductive networks [Dhand, Arya, Singh, Singh, Datta, and Malhotra (2008); Shokrieh and Rafiee (2010)]. In addition, the CNTs are dispersed in random directions when they are incorporated in the matrix, and the random orientation of CNTs may accelerate the entanglement and agglomeration of nanotubes [Shi, Feng, Huang, Hwang, and Gao (2004)].

To date, the electrical properties of nanocomposites containing CNTs have been widely studied with experimental and theoretical approaches. The electrical conductivity of single-walled CNT (SWNT)/polymer composites was investigated by Ramasubramaniam, Chen, and Liu (2003), and substantial improvements in the electrical characteristics of nanocomposites with low contents of SWCNTs were documented in their study. In addition, influences of the dispersion state and the aspect ratio of CNTs on the percolation threshold of nanocomposites reinforced with CNTs were investigated by Li, Ma, Chow, To, Tang, and Kim (2007). They reported that the critical factors determining the electrical performance of nanocomposites include: the aspect ratio, the entanglement phenomenon, and the distribution level of CNTs [Li, Ma, Chow, To, Tang, and Kim (2007)]. Seidel and Lagoudas (2009) developed a micromechanical model based on the Mori-Tanaka method [Mori and Tanaka (1973); Hiroshi and Minoru (1986)] and the composite cylinders approach [Hashin (1990)] for nanocomposites reinforced by CNTs. They treated the interphase layer between the matrix and CNTs as an external boundary, which is a hopping electron mechanism [Seidel and Lagoudas (2009)].

More recently, a micromechanical analysis based on the Ponte Castañeda-Willis (PCW) model [Castañeda and Willis (1995)] was performed by Weng (2010) to address the effect of CNT orientation on the electrical conductivity and percolation threshold of nanocomposites. Feng and Jiang (2013) also proposed a mixed micromechanical model to predict the overall electrical characteristics of CNT-reinforced nanocomposites. It was found that the conductive network significantly affects the electrical performance of the composites, and the aspect ratio of CNTs

is one of the most critical factors on the percolation threshold of the composite materials. A number of numerical analyses of microstructures in heterogeneous materials have also been carried out [Bishay and Atluri (2013); Dong, Alotaibi, Mohiuddine, and Atluri (2014)].

On the basis of the aforementioned researches, consideration of CNT entanglement, which is significantly related to the distribution of CNTs, is essential to precisely predict the electrical characteristics of nanocomposites [Yang, Souri, Kim, Ryu, and Lee, 2014]. Nevertheless, only a few studies have rigorously investigated the effects due to their complex nature. In the present study, the micromechanics-based PCW model [Weng (2010)] is utilized to investigate the electrical conductivity and percolation threshold of nanocomposites and to address the agglomeration and entanglement mechanisms of CNTs. CNTs ranging from straight to fully entangled nanotubes are assumed to be ellipsoidal inclusions, which are dependent on the aspect ratio of the nanotubes. In addition, the distribution of CNTs embedded in the matrix materials is assumed to obey a logarithmic normal function.

A series of parametric studies considering various shapes and curviness distributions of CNTs are carried out to evaluate the effects of entanglement on the electrical performance of nanocomposites. Comparisons between experimental results [Ahmad, Pan, and Shi (2006); Li, Huang, Du, He, Lin, Gao, Ma, Li, Chen, and Eklund (2006)] and the present predictions are made to evaluate the predictive capability of the proposed model. Furthermore, the present model is incorporated into the commercial finite element (FE) software HFSS (High Frequency Structure Simulator) [ANSYS HFSS (2008)] to simulate the electromagnetic shielding effectiveness (EMI) of nanocomposites.

2 Modeling of entangled CNTs embedded in a matrix

Due to the high aspect ratio of nanotubes and the resin viscosity, the CNTs embedded in a matrix are often observed to be curved and looped rather than straight [Fiedler, Gojny, Wichmann, Nolte, and Schulte (2006)]. Curved CNTs may lead to an inhomogeneous distribution within the matrix material, and it ultimately interferes with the formation of an effective conductive path, as shown in Fig. 1 [Shi, Feng, Huang, Hwang, and Gao (2004); Cha, Kim, Lee, Mo, and Hong (2005)]. Since the overall electrical performance of the nanocomposite is dominated by the conductive network, the influence of the entanglement mechanism on CNT agglomeration is a critical issue and should be carefully investigated [Izadi and Kadir (2010); Pan, Weng, Meguid, Bao, Zhu, and Hamouda (2011)].

However, it would be difficult to quantify the level of agglomeration in composites since the experimental measurement of each CNT shape is quite challenging [Sin-

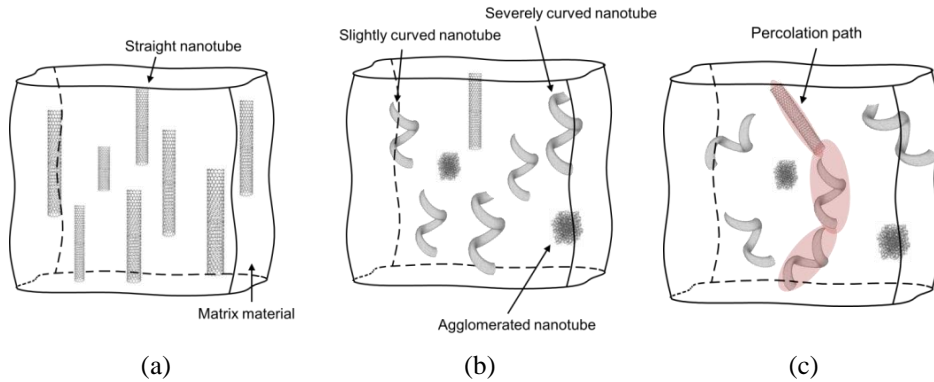


Figure 1: Schematic representations of a composite showing the effects of nanotube curviness and orientation on the filler connectivity: nanocomposites containing (a) unidirectionally aligned straight CNTs, (b) unidirectionally aligned and curved CNTs, and (c) 3D randomly oriented and curved CNTs.

nott, Mao, and Lee (2002); Li, Thostenson, and Chou (2008)]. To overcome this challenge, the CNTs within the matrix are considered as an ellipsoidal inclusion and the degree of CNT curviness is assumed to be affected by the spiral (θ) and the polar angle (ψ) in the present study (Fig. 2). Hence, the relation between the aspect ratio (α) and the curviness degree of CNTs can be determined as follows [Shi, Feng, Huang, Hwang, and Gao (2004)]:

$$\alpha = \frac{L^E}{d^E} = \frac{\psi}{2 \cos \theta} \tag{1}$$

where L^E and d^E denote the effective length and diameter of the curved nanotube, respectively; θ and ψ are the spiral and polar angle, respectively; H and d^O are the partial height and the diameter of CNTs, respectively (Fig. 2) [Shi, Feng, Huang, Hwang, and Gao (2004)].

Due to the vdW attraction between adjacent tubes [Ajayan, Schadler, Giannaris and Rubio (2001)], CNTs become more entangled by adhering to each other when their curviness becomes more severe than a specific criterion. Hence, when the partial height (H) is equal or less than the nanotube diameter (d^O), the CNTs are regarded as entangled nanotubes (agglomeration) in the present study. The agglomeration is then separately treated as sphere-shape inclusions, and the criterion between curved and entangled CNTs can be defined as given below (see, Fig. 3).

$$H = \pi d^E \tan \theta \leq d^O \quad (\text{when } \psi \geq 2\pi) \tag{2}$$

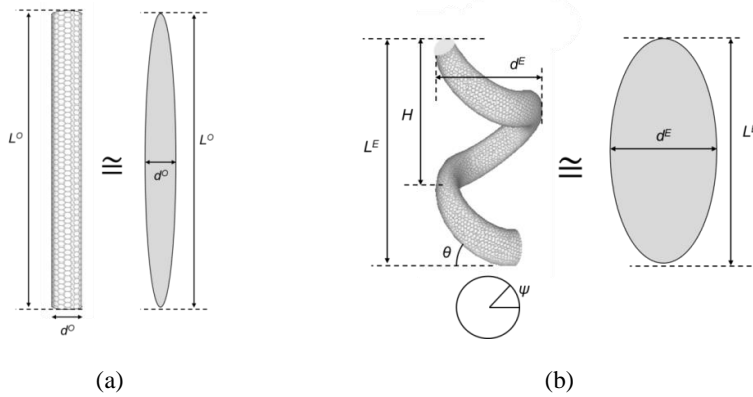


Figure 2: Schematic of the effective ellipsoidal inclusions used to model the electrical conductivity of the carbon nanotube embedded in composites: (a) the straight nanotube and (b) the curved nanotube.

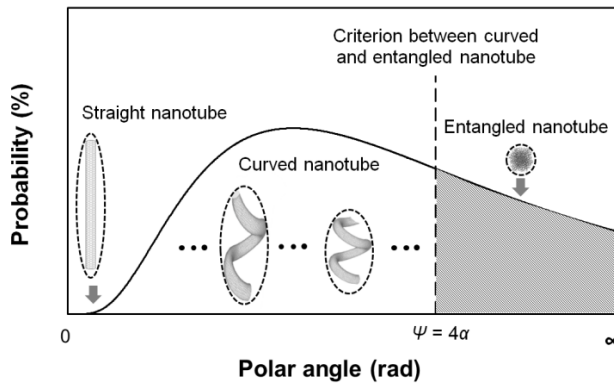


Figure 3: Schematic illustration of the proposed approach.

with

$$d^O = \frac{\psi d^E}{2\alpha \cos \theta} \tag{3}$$

The criterion that determines the entangled CNT can then be derived as

$$2\pi\alpha \sin \theta \leq \psi \quad \text{for} \quad 0 < \theta < \frac{\pi}{2} \tag{4}$$

From Eq. (4), it is noted that the spiral (θ) and polar angle (ψ) are the only undetermined variables since the aspect ratio of CNT (α) is a value that can be measured by experiment.

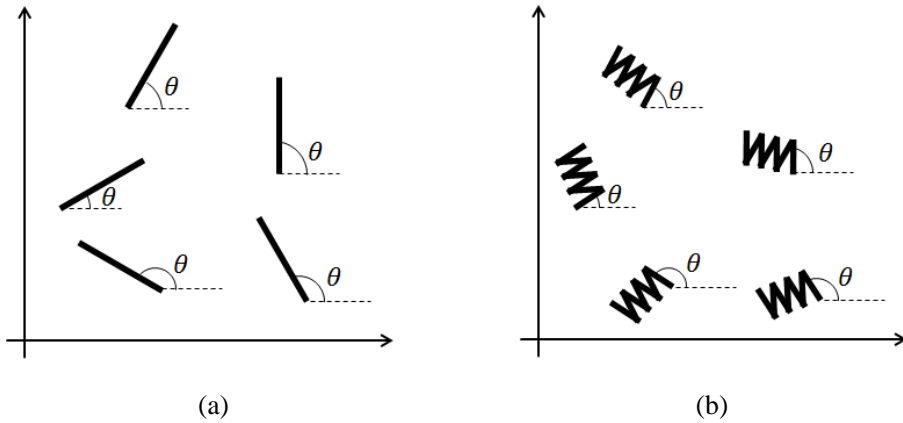


Figure 4: Dispersed direction of straight CNTs and waved CNTs with spiral angle variable.

In addition, the spiral angle is an independent constant in the fixed Cartesian coordinate system, and is not affected by the polar angle when the nanotube is randomly and uniformly distributed (Fig. 4). Thus, the variable of the spiral angle can be simplified by taking the average method as

$$\bar{f}(\theta) = \frac{2}{\pi} \int_0^{\frac{\pi}{2}} \sin\theta d\theta \tag{5}$$

From Eqs. (2)-(5), the criterion between curved and entangled CNTs can be derived by one variable, the polar angle, as follows.

$$4\alpha \leq \psi \tag{6}$$

The polar angle is assumed to have a log-normal distribution in the proposed model [Andreescu, Savin, Steigmann, Iftimie, Mamut, and Grimberg (2008); Ciecierska, Boczkowska, and Kurzydowski (2010)], and thus the probability density function of the distribution is described as [Spanoudaki and Pelster (2001)]

$$f(\psi; \mu; s) = \frac{1}{\psi s \sqrt{2\pi}} \exp \left[-\frac{(\ln \psi - \mu)^2}{2s^2} \right] \tag{7}$$

where μ is the mean value and s is the standard deviation, which signifies the curviness distribution of CNTs, respectively. A CNT with $\psi = 0$ is considered to be a straight tube, while a CNT with a larger polar angle than the criterion ($4\alpha \leq \psi$) is regarded as an entangled nanotube that has an approximately spherical shape.

3 Recapitulation of PCW model for effective electrical conductivity of nanocomposites with entanglement effects

The Ponte Castañeda-Willis (PCW) model [Castañeda and Willis (1995); Weng (2010)] is adopted here to predict the effective electrical conductivity of nanocomposites containing CNTs. For the completeness of the proposed approach, the PCW model [Weng (2010)] is briefly recapitulated here.

The most distinguished feature of the PCW model is to consider multi-phase inclusions with different shapes [Weng (2010)], allowing incorporation of the entanglement mechanism into the framework. In addition, the PCW model features a simple closed form that can be modified and extended to a more realistic schema by means of computational modelling [Pan, Weng, Meguid, Bao, Zhu, and Hamouda (2011)]. Let us consider a q -phase composite ($q=0, 1, \dots, n$) consisting of a matrix (phase 0) with electrical conductivity \mathbf{L}_0 , and initially straight CNTs (phase 1) with electrical conductivity \mathbf{L}_1 . The CNTs could be looped when the nanotubes are incorporated into the matrix, and the curved CNTs with varying degree of curviness are separately regarded as different phases. Hence, the analytical model for the prediction of aligned CNT-reinforced nanocomposites with the entanglement effect can be written as [Weng (2010)]

$$\mathbf{L}_{Aligned}^* = \mathbf{L}_0 + \left[\mathbf{I} - \sum_{q=1}^n (\phi_q \mathbf{T}_q \cdot \mathbf{S} \cdot \mathbf{L}_0)^{-1} \right]^{-1} \cdot \left[\sum_{q=1}^n (\phi_q \mathbf{T}_q) \right] \quad (8)$$

with

$$\mathbf{T}_q = \left[(\mathbf{L}_q - \mathbf{L}_0)^{-1} + \mathbf{S} \cdot \mathbf{L}_0^{-1} \right]^{-1} \quad (9)$$

where \mathbf{L}_q and ϕ_q are the electrical conductivity and the volume fraction of the q -phase ($q=0, 1, \dots, n$); \mathbf{S} denotes the Eshelby tensor, which is a spheroidal inclusion with a symmetric axis 3 as [Landau, Bell, Kearsley, Pitaevskii, Lifshitz, and Sykes (1984); Pan, Weng, Meguid, Bao, Zhu, and Hamouda (2011)]

$$S_{11} = S_{22} = \begin{cases} \frac{\alpha}{2(\alpha^2-1)^{1.5}} \left[\alpha (\alpha^2 - 1)^{0.5} - \cosh^{-1} \alpha \right], & \alpha > 1 \\ \frac{\alpha}{2(1-\alpha^2)^{1.5}} \left[\cos^{-1} \alpha - \alpha (1 - \alpha^2)^{0.5} \right], & \alpha < 1 \end{cases} \quad (10)$$

$$S_{33} = 1 - 2S_{22}$$

where α is the aspect ratio of CNTs (length-to-diameter ratio) that is defined as $\alpha=L^E/d^E$ in Eq. (1). With the spherical-shaped inclusion, Eq. (10) reduces to $S_{11} = S_{22} = S_{33}=1/3$ [Pan, Weng, Meguid, Bao, Zhu, and Hamouda (2011)]. Note

that the conductivity value of CNTs is assumed to be identical regardless of the curviness level in the present study.

In addition, the analysis for nanocomposites containing aligned CNTs can then be extended to the condition of randomly oriented nanotubes, and it is explicitly written as [Weng (2010)]

$$\mathbf{L}_{3D}^* = \mathbf{L}_0 + \left[\mathbf{I} - \sum_{q=1}^n (\phi_q \bar{\mathbf{T}} \cdot \mathbf{L}_0)^{-1} \right]^{-1} \cdot \left[\sum_{q=1}^n (\phi_q \bar{\mathbf{T}}) \right] \quad (11)$$

The component $\bar{\mathbf{T}}$ and explicit solution of the model in Eq. (11) are given in [Pan, Weng, Meguid, Bao, Zhu, and Hamouda (2011)]. The Hashin-Shtrikman (HS) bounds are also applied to the present model when the predicted effective conductivities exceed the theoretical limitations [Pan, Weng, Meguid, Bao, Zhu, and Hamouda (2011)] A more detailed description of PCW model for effective electrical conductivity of nanocomposites can be found in [Weng (2010); Pan, Weng, Meguid, Bao, Zhu, and Hamouda (2011)].

As shown in Fig. 3, the level of CNT curviness becomes more intense as the polar angle increases. The effective aspect ratio of CNTs is thus variable with respect to the polar angle, and different shapes of ellipsoidal inclusions would be embedded in the matrix material. In the model proposed by Pan et al. (2001), CNTs embedded in the composites are assumed to be perfectly straight. However, the incorporated nanotubes are often observed to be curved rather than being straight [Gojny, Wichmann, Köpke, Fiedler, and Schulte (2004); Tsai, Zhang, Jack, Liang, and Wang (2011)], and thus the present proposed model is expected to enable the more realistic simulation of CNTs-reinforced nanocomposites. However, it should be noted that the influence of CNT waviness tends to be insignificant as the volume fraction of CNT increases. Fig. 5 shows the algorithm for predicting the electrical behavior of nanocomposites with the curviness effect.

In the algorithm presented in Fig. 5, the materials properties (\mathbf{L}_q and α) and the log-normal distribution constants (μ , s) must be identified. Here, μ is assumed to be $\log(\alpha)$ based on the literatures [Andreescu, Savin, Steigmann, Iftimie, Mamut, and Grimberg (2008); Ciecierska, Boczkowska, and Kurzydowski (2010)], and s is set to be an intrinsic property that is dependent on the material constituents. Here, increment of the polar angle is 1 rad ranging uniformly from 0 to the criterion.

Since the CNT with $4\alpha \leq \psi$ is considered as a sphere-shaped inclusion, the number of phases in the matrix increases until the polar angle exceeds the criterion. Considering the correlations between the polar angle and the aspect ratio of CNTs, the effective electrical conductivities are calculated and updated simultaneously with an increasing polar angle value. In addition, the symbols adopted in Fig. 5 are

clearly explained in Table 1.

Table 1: The symbols adopted in the interactive algorithm for the electrical conductivity simulation.

Symbol	Description
L_q	Electrical conductivity of q -phase
ϕ_q	Volume fraction of CNTs of q -phase
μ	Mean value of log-normal distribution
s	Standard deviation of log-normal distribution
α	Aspect ratio of CNTs (length-to-diameter)
\mathbf{S}	Eshelby tensor (Pan et al., 2011)
θ	Spiral angle of CNT
ψ	Polar angle of CNT

4 Parametric study on the distribution effect of CNTs

Based on the present proposed model, a series of numerical simulations is performed to elucidate the effects of the CNT curviness and entanglement on the electrical conductivity of nanocomposites. Since the aspect ratio and the orientation of CNTs are expected to considerably affect the percolation behavior [Li, Ma, Chow, To, Tang, and Kim (2007)], influences of the parameters are also investigated through the numerical study. The CNT/alumina composite manufactured by Ahmad, Pan, and Shi (2006) is considered for the simulation, and the material properties of the matrix and CNTs are as follows: $L_0=1 \cdot 10^{-12}$ S/m, $L_1=6 \cdot 10^2$ S/m, and $\alpha=100$, respectively [Ahmad, Pan, and Shi (2006)], where L_q ($q = 0, 1$) denotes the electrical conductivity of the q -phase and α is the aspect ratio of the CNTs.

First, the simulation results with respect to CNT orientation and length are presented in Fig. 6. From the result, the electrical percolation threshold is rapidly initiated when the CNTs are 3D randomly oriented rather than unidirectionally aligned. It is also shown that the electrical path is formed earlier as increases. Hence, the present predictions reveal that the composites reinforced by 3D randomly oriented and lengthy CNTs have a higher probability of forming an electrical path compared to the aligned and short CNT-reinforced composites [Li, Ma, Chow, To, Tang, and Kim (2007); Nam, Lee, and Jang (2011)].

The influence of the CNT entanglement on the overall electrical performance of the nanocomposite is simulated, as shown in Fig. 7. In the numerical study, the

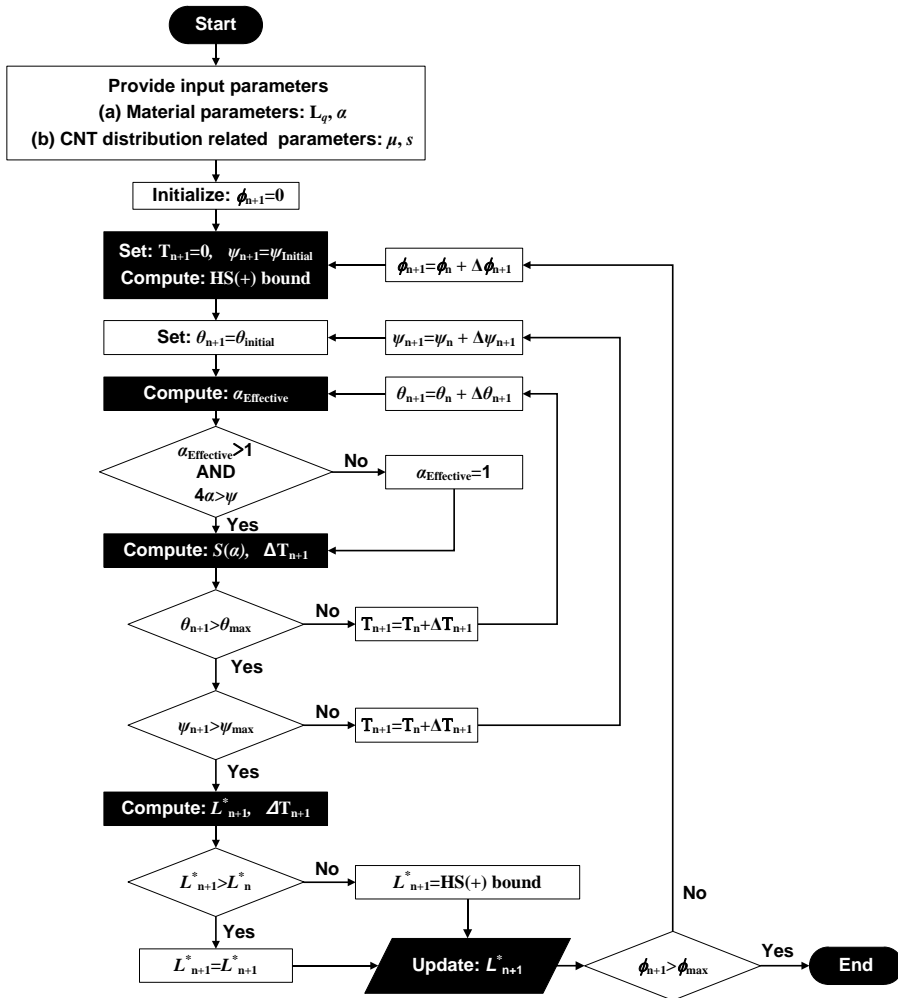


Figure 5: The recursive and interactive algorithm for the electrical conductivity simulation.

log-normal distribution parameters μ and s , which are the mean and the curviness distribution of CNTs, are assumed to be $\mu = \log(\alpha)$ and $s = 1$, respectively. Furthermore, the criterion between curved and entangled CNTs is set to be $4\alpha \leq \psi$, as derived in the previous section. Fig. 7(a) shows that an effective conductive path is formed slowly with entanglement, and therefore the overall electrical performance of the given material is predicted to be decreased. It is clear from Fig. 7(a) that the CNT entanglement is quite sensitive to the aspect ratio, and the level of agglomera-

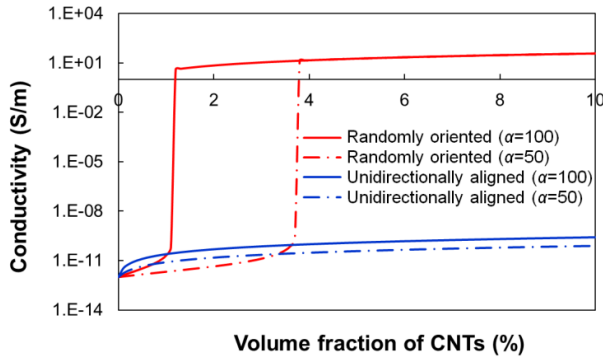
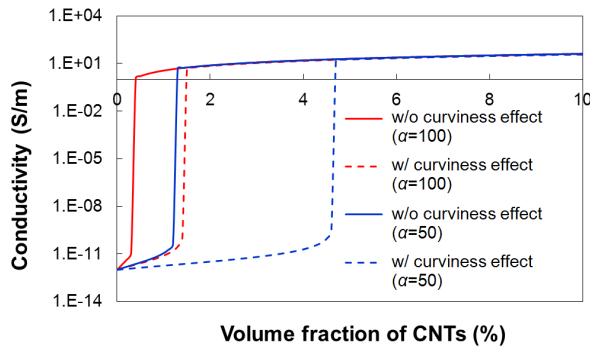
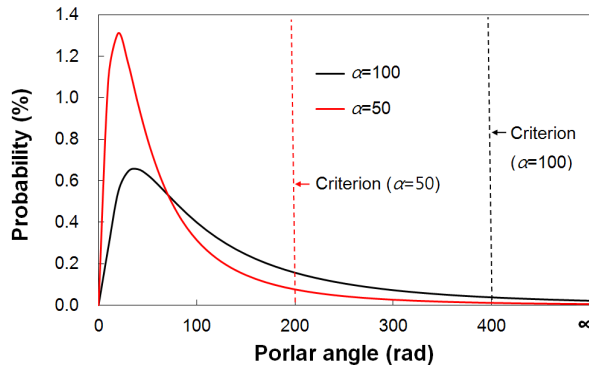


Figure 6: Effects of the nanotube orientation and length on the overall electrical conductivity of nanocomposites.



(a)

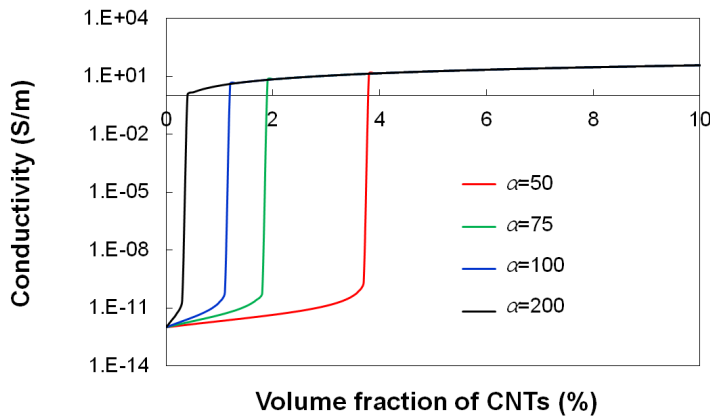


(b)

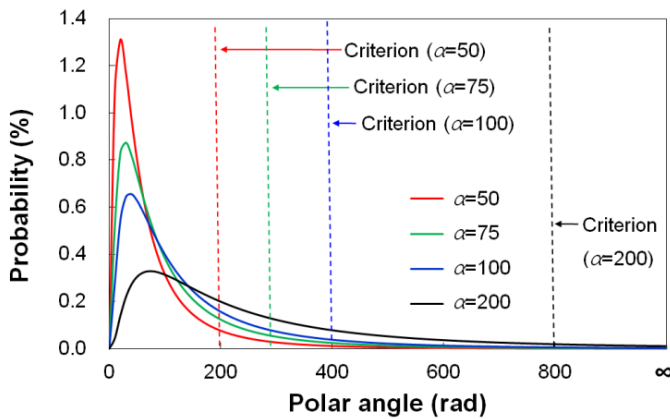
Figure 7: (a) The predicted electrical conductivity of CNT/aluminum composites with respect to the aspect ratio and the curviness effect and (b) the distribution probability of straight CNTs in the matrix corresponding to (a)

tion becomes more pronounced as the aspect ratio of the nanotubes decreases. The distribution of CNT curviness corresponding to Fig. 7(a) is depicted in Fig. 7(b).

To investigate the effect of aspect ratio on the electrical performance of the nanocomposites, the electrical conductivity with varying aspect ratios are illustrated in Fig. 8(a). It is observed from Fig. 8(a) that the incorporation of lengthy CNTs leads to an earlier percolation threshold; however, a higher aspect ratio results in more frequent occurrence of curved CNTs. In addition, the corresponding probability function of the CNTs distribution with various aspect ratios is shown in Fig. 8(b).



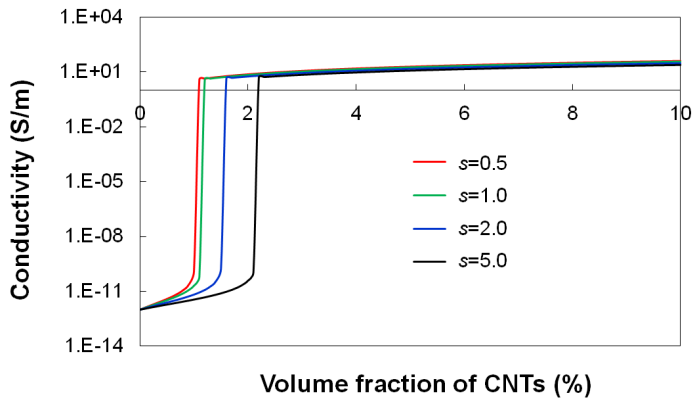
(a)



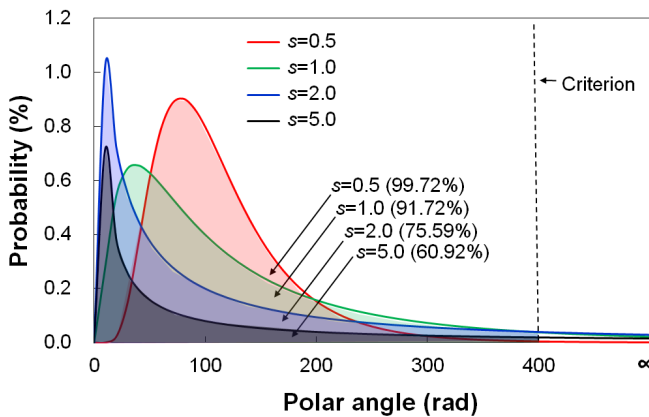
(b)

Figure 8: (a) The predicted conductivity of nanocomposites against volume fraction of CNTs for different aspect ratio and (b) the probability function of the CNTs distribution with various aspect ratios.

A parametric analysis of the curviness distribution, s , is conducted in accordance with the polar angle, as shown in Fig. 9. The aspect ratio of CNTs is fixed to be $\alpha=100$, and four values of the distribution parameter are considered: 0.5, 1.0, 2.0, and 5.0. It can be seen from Fig. 9(a) that the CNT agglomeration has a considerable influence on the percolation threshold, and a lower value of s leads to better electrical performance of the nanocomposites. Fig. 9(b) shows the predicted distribution of nanotubes with different parameter s corresponding to Fig. 9(a). For the CNT distribution, the probability of existence of moderate CNTs within the matrix is 99.72 % for $s=0.5$, while it is 60.92 % for $s=5.0$ (Fig. 9(b)).



(a)



(b)

Figure 9: (a) The electrical conductive properties of nanocomposites predicted by the proposed model and (b) the corresponding predicted distribution of nanotube as function of polar angle.

5 Experimental comparisons on electrical conductivity properties

Comparisons between the experimental results and the present predictions are made to evaluate the predictive capability of the proposed model. Two sets of experimental data that are available in the literature are considered for the comparisons, and the influence of CNT contents on the effective electrical conductivity of nanocomposites is discussed here. Since the model parameter, s , of the proposed model is not reported, the parameter is estimated by fitting the experimentally obtained electrical conductivity curve [Ahmad, Pan, and Shi (2006); Li, Huang, Du, He, Lin, Gao, Ma, Li, Chen, and Eklund (2006)] with the prediction. First, the electrical conductivities of alumina/multiwalled CNT (MWCNT) composites with different MWNT contents measured by Ahmad, Pan, and Shi (2006) is considered. Taking data from the literature, the material properties of the constituent phases are: $L_0=1 \cdot 10^{-12}$ S/m, $L_1=6 \cdot 10^2$ S/m, and $\alpha=100$, respectively [Ahmad, Pan, and Shi (2006); Pan, Weng, Meguid, Bao, Zhu, and Hamouda (2011)]. Here, L_0 and L_1 denote the electrical conductivity of the matrix and CNTs, respectively; α is the aspect ratio (length/diameter) of the nanotubes, and the CNT distribution parameters are set to be $\mu=\log(\alpha)$ and $s=1.0$.

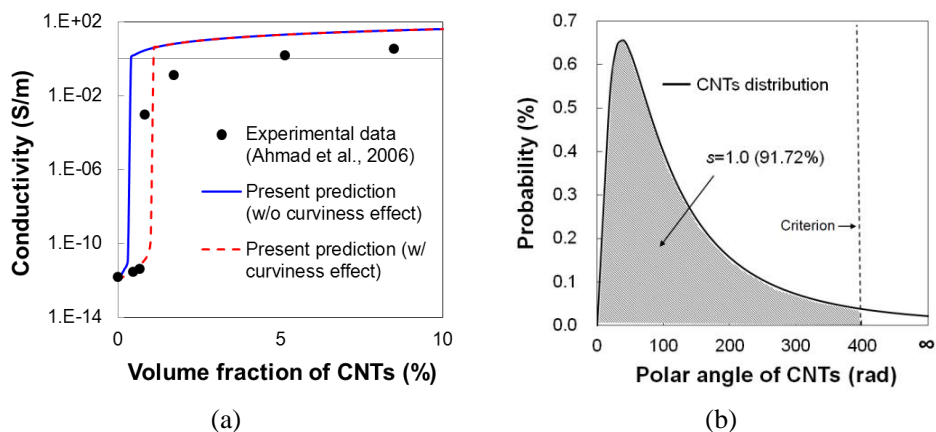


Figure 10: (a) Comparison between the proposed electrical conductivity prediction and experimental data (Ahmad et al., 2006) and (b) the corresponding predicted CNTs distribution embedded in the matrix.

Figure 10 shows comparisons of electrical conductivity from the experiment [Ahmad, Pan, and Shi (2006)] and the present prediction with different volume fractions of CNTs. The dash and solid lines correspond to the current predictions with and without the agglomeration effect, while the black dots denote the experimen-

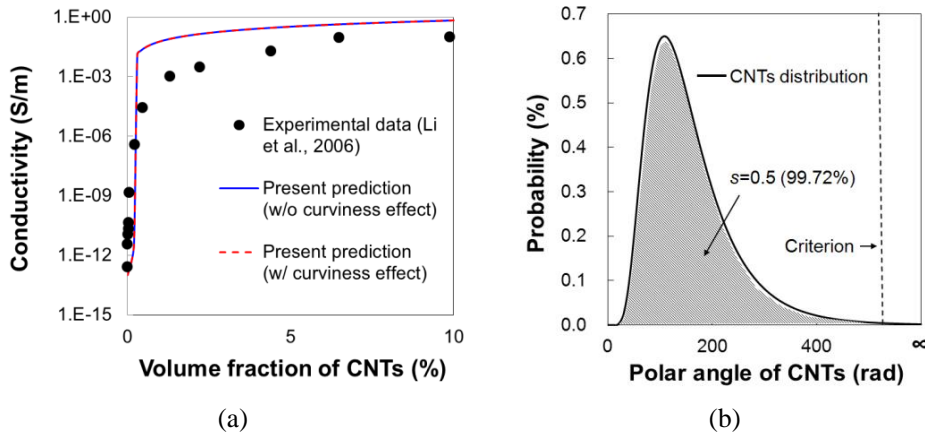


Figure 11: (a) Comparisons of the electrical conductivity with the experimental data (Li et al., 2006) and the present prediction for CNT/epoxy composites and (b) the predicted nanotube distribution as a function of the polar angle of the CNTs corresponding to (a).

tal measurements. It is found from Fig. 10(a) that the electrical conductivity of the composites increases as the volume fraction of the CNTs increases, which significantly rises from $1 \cdot 10^{-11}$ to 1.0 S/m for 1.0~1.5 % of CNTs. The predictions considering the agglomeration mechanism are lower than those without considering the agglomeration phenomena, and the predictions are thereby in good agreement with the experimental data. The predicted CNTs distribution corresponding to Fig. 10(a) is depicted in Fig. 10(b).

The predicted conductivity and the corresponding experimental data for the CNT/epoxy composite [Li, Huang, Du, He, Lin, Gao, Ma, Li, Chen, and Eklund (2006)] are shown in Fig. 11 as a function of the nanotube content. The material properties are adopted herein from Li, Huang, Du, He, Lin, Gao, Ma, Li, Chen, and Eklund (2006) as: $L_0=1 \cdot 10^{-13}$ S/m, $L_1=1 \cdot 10$ S/m, and $\alpha=139$. Overall, the present predictions match the experimental data well; however, it is observed that the agglomeration effect is not influential in the case of the CNT/epoxy composite specimens. This result may be caused by an effective distribution method that utilizes an ultrasonic machine and acetone catalyst [Li, Huang, Du, He, Lin, Gao, Ma, Li, Chen, and Eklund (2006)], and more detailed distribution and fabrication methods of the nanocomposite are described in Li, Huang, Du, He, Lin, Gao, Ma, Li, Chen, and Eklund (2006). The CNT distribution as a function of the polar angle of the nanotube corresponding to Fig. 11(a) is presented in Fig. 11(b). The predictive capability of the proposed model over the CNT content ranging from 0 to 10 % is

verified by the comparison between experimental results and calculated electrical conductivity characteristics.

6 FE simulations for prediction of the electromagnetic shielding effectiveness

Since the conductivity characteristic affects the EMI wave shielding mechanism [Chung (2001)], the shielding effectiveness of CNT-reinforced epoxy nanocomposites [Li, Huang, Du, He, Lin, Gao, Ma, Li, Chen, and Eklund (2006)] is additionally investigated in the present study. Nanocomposites with different CNTs content [Li, Huang, Du, He, Lin, Gao, Ma, Li, Chen, and Eklund (2006)] are considered for the shielding effectiveness simulation, and the commercial FE software HFSS [ANSYS HFSS (2008)] is utilized for the simulation. Fig. 12 shows the layout of modeling compositions for prediction of the EMI shielding effectiveness. In order to model the actual waveguide system, the boundary condition is designed as the wave port with a definite integration line [Codecasa and Trevisan (2010); Kwon, Kim, and Lee (2011)].

The 3D meshes for the simulation are built by reflecting the features shown in Fig. 12, and the representative electric field distributions are plotted in Fig. 13. In particular, Fig. 13(b) shows the differences in the electric distribution field as the electromagnetic wave passes through the shielding composites. The red color denotes higher intensity of the electric field [Kwon and Lee (2009)], and the applied frequency ranges from 1.5 to 1500 MHz by following the conditions reported in Li, Huang, Du, He, Lin, Gao, Ma, Li, Chen, and Eklund (2006).

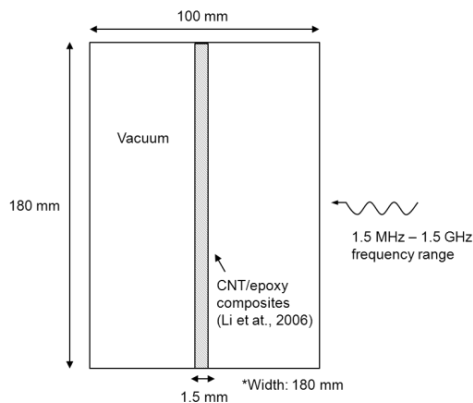


Figure 12: Layout of modeling compositions for prediction of the electromagnetic interference (EMI) shielding effectiveness (SE).

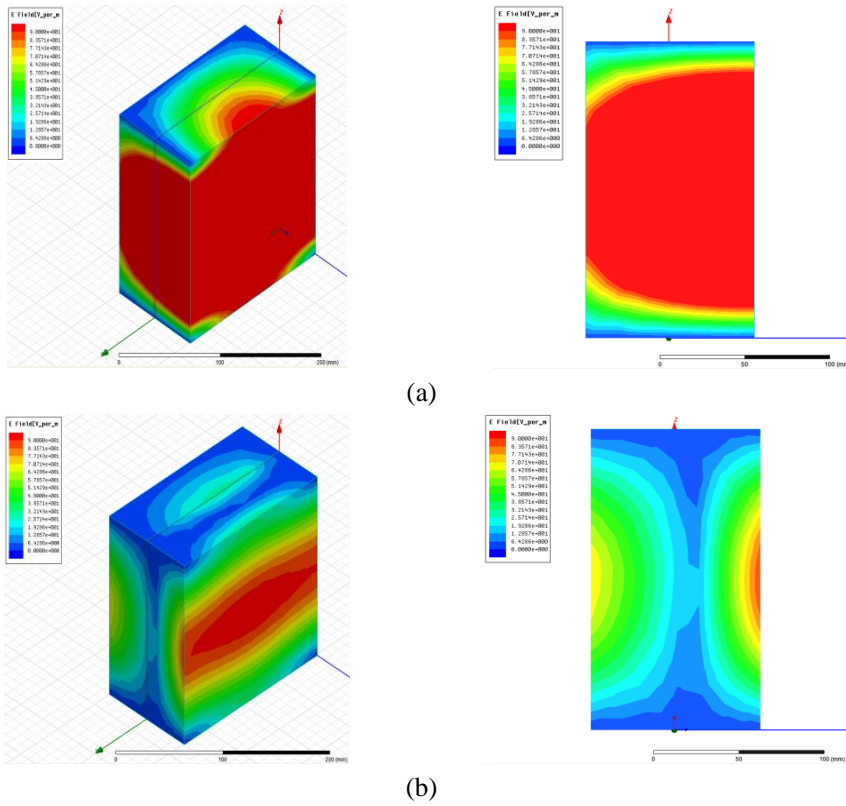


Figure 13: The predicted distributions of electric field for (a) vacuum and (b) CNT/epoxy composites.

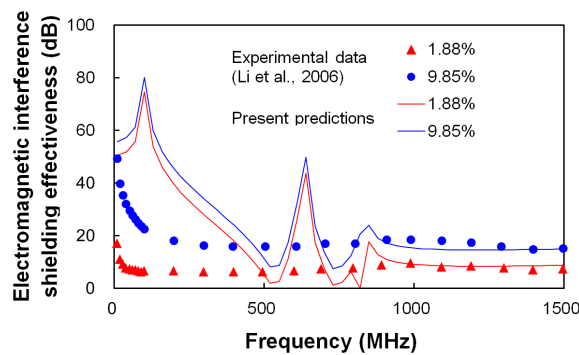


Figure 14: Comparisons of the electromagnetic interference shielding effectiveness of CNTs-reinforced nanocomposites between the present predictions and experimental data [Li et al. (2006)]

Fig. 14 shows comparisons of the EMI shielding effectiveness of CNT-reinforced nanocomposites between the present predictions and experimental data [Li, Huang, Du, He, Lin, Gao, Ma, Li, Chen, and Eklund (2006)]. Divergences from the experiment at initial frequency values (1.5~750 MHz) are observed; however, the predicted shielding effectiveness over the frequency range from 750 to 1500 MHz match well with the measurements. It may be caused by the convergence error of the FE solution [Moussakhani, McCombe, and Nikolova (2014)] and/or the simulation limitations on the environmental and boundary condition modeling [Mramor, Vertnik, and Šarler (2013); Stegeman, Pfeiffenberger, Bailey, and Hamilton (2014)]. These results provide a starting point for evaluating EMI shielding effectiveness of CNT-reinforced nanocomposites with agglomeration effects, and further theoretical study is needed in the future for a more accurate prediction on the electrical behavior of nanocomposites.

7 Concluding remarks

An analysis of randomly oriented CNTs-reinforced nanocomposites is conducted to predict the electrical performances of the composites. CNT entanglement induced by the high aspect ratio of nanotubes and the vdW force is considered [Ajayan, Schadler, Giannaris, and Rubio (2001)], and an interactive algorithm is developed to combine the entanglement mechanism in the micromechanical framework [Castañeda and Willis (1995); Weng (2010)]. Based on the statistically predicted CNT distribution, the entanglement criterion and the effective electrical conductivity are calculated. The capability of the present computational model is demonstrated via various parametric studies and comparisons with available experimental data [Ahmad, Pan, and Shi (2006); Li, Huang, Du, He, Lin, Gao, Ma, Li, Chen, and Eklund (2006)]. In addition, the present model is incorporated into the commercial FE software HFSS [ANSYS HFSS (2008)] to simulate the EMI shielding effectiveness of nanocomposites. From the present study, the following salient features are found.

- The electrical conductivities gradually rise until the predicted percolation threshold point; thereafter the rate of change is very steep with an increase of the CNT contents.
- The aspect ratio of CNTs is a very important factor influencing the entanglement criterion, and the conductivity reduction caused by the entanglement effect becomes more influential as the aspect ratio decreases.
- The incorporation of lengthy CNTs leads to an earlier percolation threshold; however, the higher aspect ratio of CNTs results in more frequent occurrence of curved CNTs.

- The effect of the aspect ratio is predicted to be heavily influential when the CNTs are oriented 3D randomly rather than when they are unidirectionally aligned.

It is worth noting that since the scope of this work is to investigate the entanglement effect on the electrical performance of CNT-reinforced nanocomposites, the curved and entangled CNTs are simply assumed to be ellipsoidal inclusions. It is believed that the limitation of the present approach can be resolved by including a new inclusion model or an additional homogenization method. In order to extensively investigate the electrical performances of nanocomposites and to examine the applicability of the present approaches in practice, additional theoretical and experimental verifications considering more parameters than those taken into account in the present study need to be carried out in the future.

Acknowledgement: This research was sponsored by the National Research Foundation of Korea (NRF) grants funded by the Korea government (NRF-2012R1A2A4 A01008855).

References

- Ahmad, K.; Pan, W.; Shi, S. L.** (2006): Electrical conductivity and dielectric properties of multiwalled carbon nanotube and alumina composites. *Appl. Phys. Lett.*, vol. 89, no. 13, pp. 133122.
- Ajayan, P. M.; Schadler, L. S.; Giannaris, C.; Rubio, A.** (2000): Single-walled carbon nanotube-polymer composites: strength and weakness. *Adv. Mater.*, vol. 12, no. 10, pp. 750-753.
- Andreescu, A.; Savin, A.; Steigmann, R.; Iftimie, N.; Mamut, E.; Grimberg, R.** (2008): Model for thermal conductivity of composites with carbon nanotubes. *J. Therm. Anal. Calorim.*, vol. 94, no. 2, pp. 349-353.
- ANSYS HFSS** (2008): *High Frequency Structure Simulation*, ANSYS Inc.
- Asgary, A. R.; Nourbakhsh, A.; Kohantorabi, M.** (2013): Old newsprint/ polypropylene nanocomposites using carbon nanotube: Preparation and characterization. *Compos. Part B-Eng.*, vol. 45 no. 1, pp. 1414-1419.
- Bishay, P. L.; Atluri, S. N.** (2013). 2d and 3d multiphysics voronoi cells, based on radial basis functions, for direct mesoscale numerical simulation (dmns) of the switching phenomena in ferroelectric polycrystalline materials. *CMC-Comput. Mater. Con.*, vol. 33, no. 1, pp. 19-62.
- Castañeda, P. P.; Willis, J. R.** (1995): The effect of spatial distribution on the effective behavior of composite materials and cracked media. *J. Mech. Phys. Solids*,

vol. 43, no.12, pp. 1919-1951.

Cha, S. I.; Kim, K. T.; Lee, K. H.; Mo, C. B.; Hong, S. H. (2005): Strengthening and toughening of carbon nanotube reinforced alumina nanocomposite fabricated by molecular level mixing process. *Scripta Mater.*, vol. 53, no. 7, pp. 793-797.

Chung, D. D. L. (2001): Electromagnetic interference shielding effectiveness of carbon materials. *Carbon*, vol. 39, no. 2, pp. 279-285.

Ciecierska, E.; Boczkowska, A.; Kurzydłowski, K. J. (2010): Quantitative description of the spatial dispersion of carbon nanotubes in polymeric matrix. *J. Mater. Sci.*, vol. 45, no. 9, pp. 2305-2310.

Codecasa, L.; Trevisan, F. (2010): Convergence of electromagnetic problems modelled by discrete geometric approach. *CMES-Comp. Model. Eng.*, vol. 58, no. 1, pp. 15-44.

Deng, F.; Zheng, Q. S.; Wang, L. F.; Nan, C. W. (2007): Effects of anisotropy, aspect ratio, and non-straightness of carbon nanotubes on thermal conductivity of carbon nanotube composites. *Appl. Phys. Lett.*, vol. 90, no. 2, pp. 021914.

Dhand, C.; Arya, S. K.; Singh, S. P.; Singh, B. P.; Datta, M.; Malhotra, B. D. (2008): Preparation of polyaniline/multiwalled carbon nanotube composite by novel electrophoretic route. *Carbon*, vol. 46, no. 13, pp. 1727-1735.

Dong, L.; Alotaibi, A.; Mohiuddine, S. A.; Atluri, S. N. (2014): Computational methods in engineering: a variety of primal & mixed methods, with global & local interpolations, for well-posed or ill-Posed BCs. *CMES-Comp. Model. Eng.*, vol. 99, no. 1, pp. 1-85.

Feng, C.; Jiang, L. (2013): Micromechanics modeling of the electrical conductivity of carbon nanotube (CNT)-polymer nanocomposites. *Compos. Part A-Appl. S.*, vol. 47, pp. 143-149.

Fiedler, B.; Gojny, F. H.; Wichmann, M. H.; Nolte, M.; Schulte, K. (2006): Fundamental aspects of nano-reinforced composites. *Compos. Sci. Technol.*, vol. 66, no. 16, pp. 3115-3125.

Gojny, F. H.; Wichmann, M. H. G.; Köpke, U.; Fiedler, B.; Schulte, K. (2004): Carbon nanotube-reinforced epoxy-composites: enhanced stiffness and fracture toughness at low nanotube content. *Compos. Sci. Technol.*, vol. 64, no. 15, pp. 2363-2371.

Hashin, Z. (1990): Thermoelastic properties and conductivity of carbon/carbon fiber composites. *Mech. Mater.*, vol. 8, no. 4, pp. 293-308.

Hiroshi, H.; Minoru, T. (1986): Equivalent inclusion method for steady state heat conduction in composites. *Int. J. Eng. Sci.*, vol. 24, no. 7, pp. 1159-1172.

Izadi, M.; Kadir, M. Z. A. A. (2010): New algorithm for evaluation of electric

fields due to indirect lightning strike. *CMES-Comp. Model. Eng.*, vol. 67, no. 1, pp. 1-12.

Kim, H. K.; Nam, I. W.; Lee, H. K. (2014): Enhanced effect of carbon nanotube on mechanical and electrical properties of cement composites by incorporation of silica fume. *Compos. Struct.*, vol. 107, pp. 60-69.

Kwon, S. H.; Lee, H. K. (2009): A computational approach to investigate electromagnetic shielding effectiveness of steel fiber-reinforced mortar. *CMC-Comput. Mater. Con.*, vol. 12, no. 3, pp. 197-221.

Kwon, S. H.; Kim, B. R.; Lee, H. K. (2011): Electromagnetic shielding effectiveness of grid-mesh films made of polyaniline: a numerical approach. *CMC-Comput. Mater. Con.*, vol. 21, no. 1, pp. 65-86.

Lahiri, D.; Ghosh, S.; Agarwal, A. (2012): Carbon nanotube reinforced hydroxypapatite composite for orthopedic application: A review. *Mater. Sci. Eng. C*, vol. 32, no. 7, pp. 1727-1758.

Landau, L. D.; Bell, J. S.; Kearsley, M. J.; Pitaevskii, L. P.; Lifshitz, E. M.; Sykes, J. B. (1984): *Electrodynamics of Continuous Media (Vol. 8)*. Elsevier.

Lau, K. T.; Gu, C.; Hui, D. (2006): A critical review on nanotube and nanotube/nanoclay related polymer composite materials. *Compos. Part B-Eng.*, vol. 37, no. 6, pp. 425-436.

Li, C.; Thostenson, E. T. Chou, T. W. (2008): Effect of nanotube waviness on the electrical conductivity of carbon nanotube-based composites. *Compos. Sci. Technol.*, vol. 68, no. 6, pp. 1445-1452.

Li, N.; Huang, Y.; Du, F.; He, X.; Lin, X.; Gao, H.; Ma, Y.; Li, F.; Chen, Y.; Eklund, P. C. (2006): Electromagnetic interference (EMI) shielding of single-walled carbon nanotube epoxy composites. *Nano Lett.*, vol. 6, no. 6, pp. 1141-1145.

Li, J.; Ma, P. C.; Chow, W. S.; To, C. K.; Tang, B. Z.; Kim, J. K. (2007): Correlations between percolation threshold, dispersion state, and aspect ratio of carbon nanotubes. *Adv. Funct. Mater.*, vol. 17, no. 16, pp. 3207-3215.

Mori, T.; Tanaka, K. (1973): Average stress in matrix and average elastic energy of materials with misfitting inclusions. *Acta Metall.*, vol. 21, no. 5, pp. 571-574.

Moussakhani, K.; McCombe, J. J.; Nikolova, N. K. (2014): Sensitivity of microwave imaging systems employing scattering parameter measurements. *IEEE T. Microw. Theory*, vol. 62, no. 10, pp. 2447-2455.

Mramor, K.; Vertnik, R.; Šarler, B. (2013): Simulation of natural convection influenced by magnetic field with explicit local radial basis function collocation method. *CMES-Comp. Model. Eng.*, vol. 92, no. 4, pp. 327-352.

Nam, I. W.; Lee, H. K.; Jang, J. H. (2011): Electromagnetic interference shielding/absorbing characteristics of CNT-embedded epoxy composites. *Compos. Part A-Appl. S.*, vol. 42, no. 9, pp. 1110-1118.

Pan, Y.; Weng, G. J.; Meguid, S. A.; Bao, W. S.; Zhu, Z. H.; Hamouda, A. M. S. (2011): Percolation threshold and electrical conductivity of a two-phase composite containing randomly oriented ellipsoidal inclusions. *J. Appl. Phys.*, vol. 110, no. 12, pp. 123715.

Ramasubramaniam, R.; Chen, J.; Liu, H. (2003): Homogeneous carbon nanotube/ polymer composites for electrical applications. *Appl. Phys. Lett.*, vol. 83, no. 14, pp. 2928-2930.

Seidel, G. D.; Lagoudas, D. C. (2009): A micromechanics model for the electrical conductivity of nanotube-polymer nanocomposites. *J. Compos. Mater.*, vol. 43, no. 9, pp. 917-941.

Shi, D. L.; Feng, X. Q.; Huang, Y. Y.; Hwang, K. C.; Gao, H. (2004): The effect of nanotube waviness and agglomeration on the elastic property of carbon nanotube-reinforced composites. *J. Eng. Mater.-T ASME*, vol. 126, no. 3, pp. 250-257.

Shokrieh, M. M.; Rafiee, R. (2010): Stochastic multi-scale modeling of CNT/polymer composites. *Comp. Mater. Sci.*, vol. 50, no. 2, pp. 437-446.

Sinnott, S. B.; Mao, Z.; Lee, H. K. (2002): Computational studies of molecular diffusion through carbon nanotube based membranes. *CMES-Comp. Model. Eng.*, vol. 3, no. 5, pp. 575-587.

Spanoudaki, A.; Pelster, R. (2001): Effective dielectric properties of composite materials: the dependence on the particle size distribution. *Phys. Rev. B*, vol. 64, no. 6, pp. 064205.

Stegeman, T.; Pfeifferberger, A. H.; Bailey, J. P.; Hamilton M. C. (2014): Broadband characterisation of engineered dielectric fluids using microstrip ring resonator technique. *Electron. Lett.*, vol. 50, pp. 576-578.

Tsai, C. H.; Zhang, C.; Jack, D. A.; Liang, R.; Wang, B. (2011). The effect of inclusion waviness and waviness distribution on elastic properties of fiber-reinforced composites. *Compos. Part B-Eng.*, vol. 42, no. 1, pp. 62-70.

Wang, Y.; Weng, G. J.; Meguid, S. A.; Hamouda, A. M. (2014): A continuum model with a percolation threshold and tunneling-assisted interfacial conductivity for carbon nanotube-based nanocomposites. *J. Appl. Phys.*, vol. 115, no. 19, pp. 193706.

Weng, G. J. (2010): A dynamical theory for the Mori–Tanaka and Ponte Castañeda–Willis estimates. *Mech. Mater.*, vol. 42, no. 9, pp. 886-893.

Yang, B. J.; Souri, H.; Kim, S.; Ryu, S.; and Lee, H. K. (2014). An analytical model to predict curvature effects of the carbon nanotube on the overall behavior of nanocomposites. *J. Appl. Phys.*, vol. 116, no. 3, pp. 033511.

